

# Testing of Paraffin-Based Hybrid Rocket Fuel Using Hydrogen Peroxide Oxidizer

Cadet First Class Timothy R. Brown\* and Major Michael C. Lydon†  
Department of Astronautical Engineering, USAFA, CO, 80841

An investigation was conducted to determine regression characteristics of paraffin-based hybrid rocket fuels at the United States Air Force Academy. Regression rates were the main focus of the study because of the historically poor performance of hybrids in this area. Five test runs were conducted with varying fuel lengths of 8.64 to 13.72 cm. The motors consisted of 95% paraffin and 5% carbon black. The mass flux rate of 84% hydrogen peroxide ranged from 111 to 162 kg/m<sup>2</sup>-s. The hydrogen peroxide traveled through a catalyst bed before decomposing into O<sub>2</sub> and steam at approximately 800 °C. The oxidizer then entered the port where it auto-ignited the fuel. This removed the need for an ignition device and thus further simplified our system. Regression rates ranged from 2.87 mm/s to 5.28 mm/s for oxidizer mass flux rate values of 111-162 kg/m<sup>2</sup> s. Higher oxidizer mass flow rates corresponded to higher regression rates. As expected, these regression rates were higher than similar tests using HTPB or even paraffin-based fuels with gaseous oxygen.

## Nomenclature

$A_t$	= area of throat, cm <sup>2</sup>
$C_{actual}^*$	= actual characteristic exhaust velocity, m/s
$C_{theoretical}^*$	= theoretical characteristic exhaust velocity, m/s
$G_{oxavg}$	= average oxidizer mass flux rate, kg/m <sup>2</sup> s
$g_o$	= gravitational acceleration, m/s <sup>2</sup>
$H_2O_2$	= hydrogen peroxide
$I_{sp}$	= specific impulse, s
$L$	= length of fuel cylinder, cm
$m_{fuel}$	= mass fuel, kg
$m_{ox}$	= mass oxidizer, kg
$\dot{m}_{total}$	= total mass flow rate, kg/s
$\dot{m}_{H_2O_2}$	= oxidizer mass flow rate, kg/s
$O/F$	= oxidizer to fuel ratio
$P_c$	= chamber pressure, kPa
$P$	= pressure, kPa
$r_i$	= initial radius, cm
$r_f$	= final radius, cm

---

\* Student, Department of Astronautical Engineering, USAFA

† Assistant Professor, Department of Astronautical Engineering, USAFA

$\dot{r}$	= regression rate, mm/s
$T$	= thrust, N
$\Delta t$	= burn time, s
$V_t$	= velocity at throat, m/s
$\zeta$	= combustion efficiency
$\rho_{fuel}$	= density of fuel, kg/cm <sup>3</sup>
$\rho_l$	= density of oxidizer, kg/cm <sup>3</sup>

## I. Introduction

TODAY there is a growing emphasis on safety, environmental cleanliness, low cost, and simplicity. Hybrid rockets offer these advantages over solid and liquid fuel rockets. Hybrid rockets are simpler and potentially cheaper than liquid fueled rockets. Simplicity translates into reliability and added safety. Other advantages offered by hybrids include lower temperature sensitivity and throttling ability. However, there is one distinct disadvantage of hybrids when compared with liquid and solid rocket motors; their low regression rates. A high regression rate is necessary for high mass flow. Mass flow translates into changes in momentum which is the basis for rocket engine thrust. This low regression rate stems from the low heat and mass transfer from the fuel surface due to a relatively detached flame zone. As a consequence, hybrid rockets usually have much lower regression rates than solid rocket motors. Thus, thrust is often lower. Many different complex port geometries and multi-port designs have been tried in order to overcome this problem. Unfortunately, this often leads to lower volumetric efficiency. This experiment aims at solving this problem by using a fuel and oxidizer combination which has potential to create higher regression rates than many existing hybrid rocket systems. Our hypothesis states that paraffin wax inherently offers high regression potential due to droplets which readily escape from a liquid layer on the surface of the fuel into the flame zone.<sup>1</sup> This flame zone is relatively detached from the fuel surface. Waves form on the liquid layer. Droplets of fuel are lifted from these low viscosity waves and can pass through the diffusion flame and react with the oxidizer. The use of hydrogen peroxide and a catalyst bed as the oxidizer offer greater added simplicity because they exclude the need for a complicated and costly igniter system. We believe hydrogen peroxide may provide a higher  $\dot{r}$  than gaseous oxygen due to a higher inlet temperature from the catalyst bed. Other advantages of hydrogen peroxide include a high specific gravity and ratio of O<sub>2</sub> to steam. Our main objective is to measure regression rates of paraffin fuel versus varying  $\dot{m}_{H_2O_2}$  rates. To characterize the regression rate,  $\dot{r}$ , we will calculate the regression rate coefficient and the regression rate exponent.

## II. Predictions

A thermochemistry computer code provided a starting point for our investigation.<sup>2</sup> We assumed frozen flow and an exit pressure of 82.7 kPa to account for our altitude. From this data we predicted  $I_{sp}$  and optimum O/F ratios based on our fuel and oxidizer of 95% paraffin, 5% carbon black fuel, and 90% pure H<sub>2</sub>O<sub>2</sub>. Figure 1 shows the result of varying the O/F ratios vs.  $I_{sp}$ . We used this graph to obtain the optimum O/F ratio which would yield the highest possible  $I_{sp}$ . This operation was repeated 5 times; once for each motor. Each case was run using our computer code at the chamber pressure that we would use for that particular motor length. The inner port diameter and

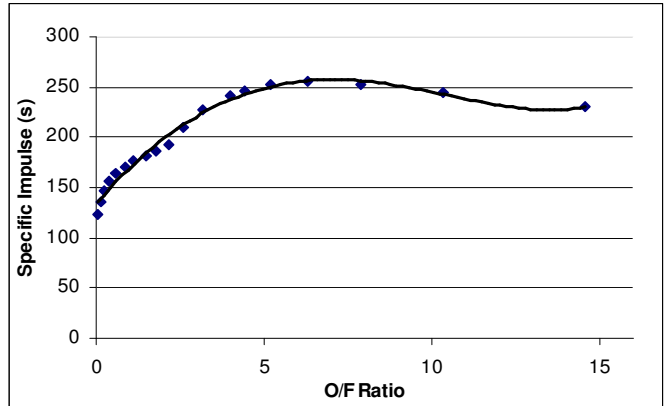


Figure 1. Specific impulse vs. O/F.

cylinder lengths were carefully measured before testing and are include below. Chamber pressures are based on  $\dot{m}_{H_2O_2}$  rates through the cavitating venturi to obtain proper O/F ratios at the maximum  $I_{sp}$ . Next, thrust levels were selected to produce the proper mass flow rates. We calculated  $\dot{m}_{H_2O_2}$  from Eq. 1c. From the thermochemistry we also calculated theoretical characteristic exhaust velocities. The  $c^*$  values in Table 1 are based on the point where  $I_{sp}$  is greatest.

Motor Number	1	2	3	4	5
Initial Mass (kg)	0.462	0.5	0.614	0.625	0.823
Initial inner port diameter (cm)	2.54	2.54	2.86	2.54	2.54
Length (cm)	8.41	8.41	10.5	10.6	13.8
Chamber Pressure (kPa)	2068.4	2068.4	3447.4	3447.4	4826.3
O/F ratio	5.8	5.8	5.8	5.8	6.31
lsp (s)	240.5	240.5	255.4	255.4	262.6
Thrust (N)	384.8	384.8	524.9	524.9	660.6
mdot ox (kg/s)	0.14	0.14	0.18	0.18	0.22
c* (m/sec)	1622	1622	1622	1622	1622

**Table 1. Predicted values.**

### III. Approach

Burn times were set at 5 seconds for conservation of  $H_2O_2$  and adequate data acquisition time. The inner radius was set at an initial value of 1.27 cm to coincide with oxidizer mass flux rates in other experiments in order to compare results. We calculated the length of the motor and  $\dot{m}_{H_2O_2}$  using the following equations:

$$\dot{m}_{total} = \frac{I_{sp}}{T g_0} \quad (1a)$$

$$\dot{m}_{fuel} = \frac{\dot{m}_{total}}{1 + O/F} \quad (1b)$$

$$\dot{m}_{ox} = \dot{m}_{total} - \dot{m}_{fuel} \quad (1c)$$

$$r_f = r_i + r \Delta t \quad (1d)$$

$$\dot{m}_{fuel} = \dot{m}_{fuel} \Delta t \quad (1e)$$

$$L = \frac{(\dot{m}_{fuel} / \rho_{fuel})}{\pi (r_f^2 - r_i^2)} \quad (1f)$$

We matched three chamber pressures of 2,068.4 kPa, 3,447.4 kPa, and 4,826.3 kPa to our fuel lengths of 8.41 cm, 10.5 cm, and 13.8 cm to obtain optimum O/F ratios.

To ensure the correct flow of oxidizer during the experiment we used a cavitating venturi. A cavitating venturi is a simple flow control device. It is a contracting and expanding nozzle which increases the flow's velocity per the

Bernoulli and continuity equation. Neglecting viscous drag, the following equations show that static pressure decreases as flow velocity increases due to the decrease in area for sub-sonic flow:

$$\frac{1}{2} \rho_1 V_1^2 + P_1 = \frac{1}{2} \rho_2 V_2^2 + P_2 \quad (2a)$$

$$\rho_1 V_1 A_1 = \rho_2 V_2 A_2 \quad (2b)$$

The velocity after the initial acceleration in the converging section is high enough to lower the static pressure below the fluid vapor pressure. The flow is then limited due to a gaseous bubble within the diverging portion of the nozzle. Thus, the flow only depends on upstream pressure and is independent of abrupt changes in pressure in the downstream chamber.

We created two graphs to relate the nitrogen pressurant pressure to the pressure just upstream of the cavitating venturi and another to relate the upstream pressure of the cavitating venturi to the mass flow of the oxidizer. We did this by timing water flow through our oxidizer system and measuring the mass afterwards on a scale. After this was completed our group predicted the oxidizer mass flow strictly from the nitrogen pressures of the pressurizing tank during the actual experiment. Figure 2 shows the calibration of the cavitating venturi. A first order linear regression yields the following equation:

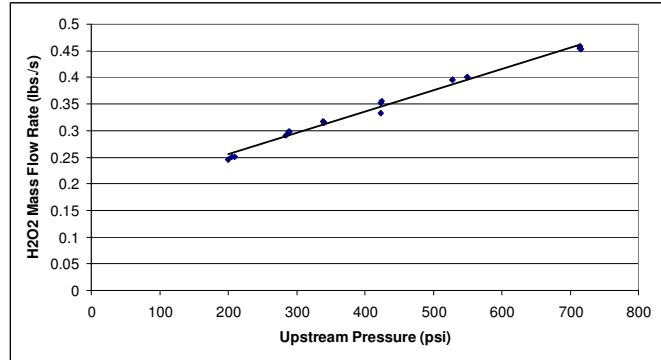


**Figure 2. HTP vs. upstream pressure.**

$$\dot{m}_{H_2O_2} = .0004 P + .01759 \quad (3)$$

#### IV. Experimental Test Set-Up

The entire system was pressurized by a 2,000 psi nitrogen tank. From this we used pressure regulators and flexible hose to pressurize our water-cooled nozzle, purge system, and oxidizer. The purge system of N<sub>2</sub> gas safely removed any excess H<sub>2</sub>O<sub>2</sub> after each test before we handled the spent fuel cartridges. The fuel cylinder was built in a manner which allowed fuel cartridges to be exchanged quickly. Each fuel cartridge also had a spacer to hold the paraffin fuel in place within the steel motor case and provide a mixing chamber aft of the Paraffin fuel.

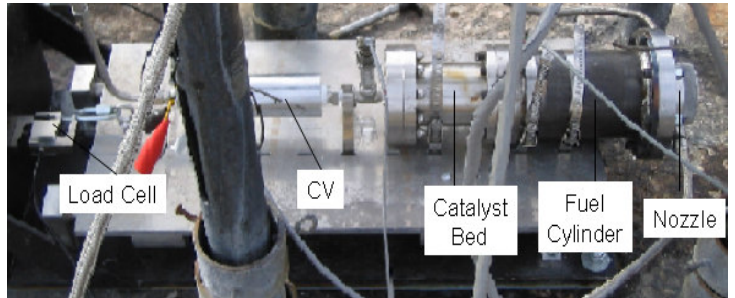


**Figure 3. Test stand.**

The water cooled nozzle and N<sub>2</sub> purge system were pressurized to 85 psi using a regulator. The water cooled nozzle worked by pumping water from one tank filled with water to another via our copper nozzle during firing. This prevented the temperature of the nozzle from reaching melting temperature. Copper was used because it readily transfers heat from the combustion products to the water. The nozzle had a 7.145 cm<sup>2</sup> exit area and a 0.7123 cm<sup>2</sup> throat area. This yielded an expansion ratio of 10.03.

The cavitating venturi was placed just ahead of the catalyst bed. It was here, in our catalyst bed, that the  $H_2O_2$  decomposed into gaseous oxygen and water at a temperature of approximately  $800^\circ\text{C}$ . The hot oxidizer immediately entered our paraffin fuel port where it auto-ignited the fuel. The data acquisition system took thrust and pressure data at 1,000 Hz.

We calibrated our load cell with weights before testing began and left a 35 lb. preload on the system. This bias can be seen in Figure 5.

We recorded pressure readings at three points; the combustion chamber, before the cavitating venturi, and immediately after the cavitating venturi.

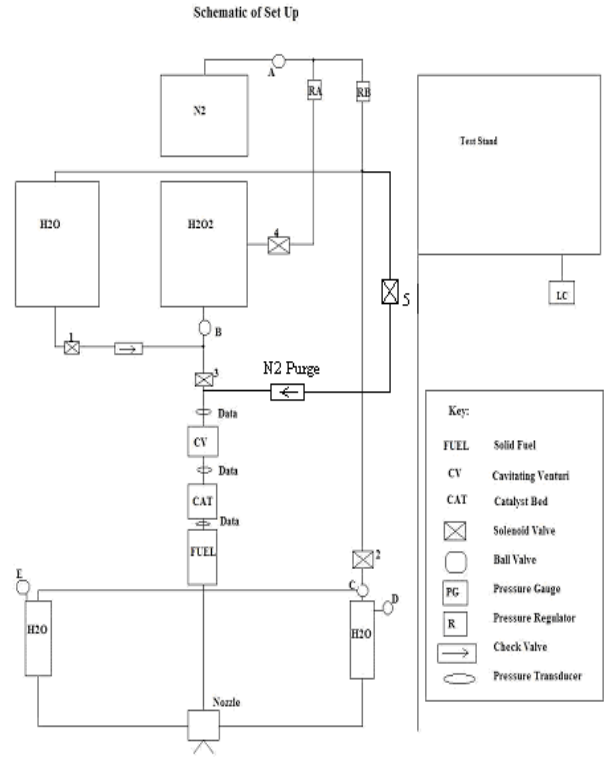


**Figure 4. Test Set-Up.**

## V. Results

Following the experiment we weighed the five motors and then measured the final web thickness. We calculated burn times from the start until the finish of fuel combustion as shown in Figure 5. Every data point in this range was averaged for an accurate average thrust reading from our 200 lb. load cell.

Chamber pressure was calculated from the point where the pressure first reached its average value during the burn until the point of the first noticeable drop off. Each of these data points was also averaged to provide an accurate measurement of average chamber pressure.

Next, we entered the pressure measured immediately before the cavitating venturi into Eq. 3 to calculate the  $H_2O_2$  flow rate. We then used Eq. 4 to calculate  $G_{oxavg}$ .

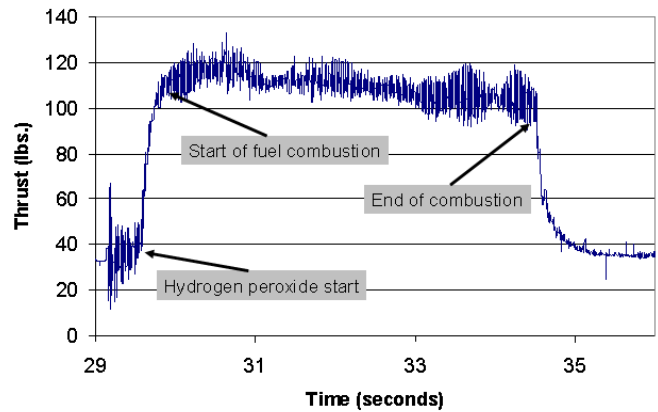


**Figure 5. Thrust result for motor 5.**

$$G_{oxavg} = \frac{\dot{m}_{ox}}{(A_{port_i} + A_{port_f})/2} \quad (4)$$

We next used the below equations to calculate the data presented on Table 2.

$$I_{sp} = \frac{T}{m g_0} \quad (5a)$$

$$c^*_{actual} = \frac{P_c A_T}{m} \quad (5b)$$

$$\zeta = \frac{c^*_{actual}}{c^*_{theoretical}} \quad (5c)$$

The following equation accurately calculates the regression rate based on cylinder geometry, measured mass change, and burn time.<sup>3</sup> We used this method to calculate our regression rates for each test case.

$$\dot{r} \approx \frac{\Delta r}{\Delta t} = \frac{\sqrt{((4(m_i - m_f) / \pi \rho_f L) + D_i^2) - D_i^2}}{2(t_f - t_i)} \quad (6)$$

To model our regression rate we chose to use a power law approximation. This equation is shown in Eq. 7. The two parameters are:  $a$ , the regression rate coefficient, and  $n$ , the regression rate exponent. The complete expression is shown below where  $G_{ox,avg}$  is in  $\text{kg/m}^2\text{-s}$ :

$$\dot{r} = a G_{ox}^n \text{ mm/sec} \quad (7)$$

$$\dot{r} = .0344 G_{ox}^{.9593} \quad (8)$$

This equation yields a regression rate exponent value of .9593 and the regression rate coefficient value of .0344.

For comparison purposes Figure 7 shows our standard regression rate result, regression rate result including a 5% mass loss, and a paraffin/Gox result by Karabeyoglu, Cantwell, and Altman.<sup>1</sup> We included a 5% mass loss because of the possibility that some of the motor sample was lost after each firing. This was because much of the



**Figure 6. Paraffin fuel after firing.**

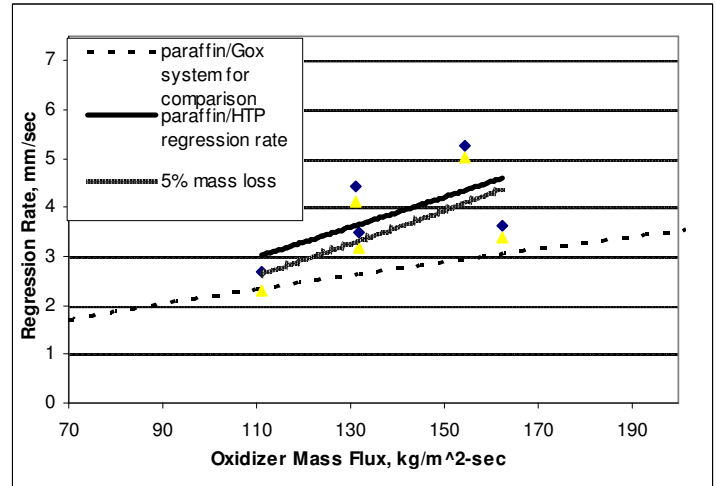


**Figure 7. Regression rate vs. oxidizer mass flux.**

wax was still in its liquid state. For our 5% mass loss assumption the regression rate exponent was 1.3338 and our regression rate coefficient was .0049. A table summarizing our results is included below.

Motor Number	1	2	3	4	5
Final Mass (kg)	0.303	0.359	0.479	0.366	0.538
Final inner port diameter (cm)	4.46	4.42	5.12	4.17	4.9
Chamber Pressure (kPa)	2120	1774	2698	2179	3114
O/F ratio	2.7	3.95	4.03	1.89	3.22
Isp (s)	97	103	151	101	136
Thrust (N)	175	170	276	220	340
mdot ox (kg/s)	0.135	0.135	0.149	0.144	0.194
c* actual (m/sec)	819	749	1032	704	872
Efficiency	0.505	0.462	0.636	0.434	0.538
rdot (mm/s)	4.43	3.5	2.87	5.28	3.63
rdot using web thickness (mm/s)	2.63	2.22	2.65	2.22	2.5
rdot assuming 5% loss of final mass (mm/s)	4.12	3.16	2.31	5.01	3.38
Gox (kg/m-s <sup>2</sup> )	131.19	131.89	111.62	154.31	162.4

**Table 2. Results.**

## VI. Conclusions

Our main objective, to measure the regression rates of paraffin fuel with varying  $H_2O_2$  oxidizer mass flow rates, was a success. The hypothesis presented earlier in this paper that paraffin-based fuel has potential to demonstrate high regression rates due to the formation of droplets of wax, which could readily enter the flame zone, was proven correct. A similar test was conducted by Stanford University using gaseous oxygen as the oxidizer and a paraffin-based fuel. They achieved regression rates of approximately 2.6 mm/sec for  $G_{oxavg}$  values of 130 kg/m<sup>2</sup>-s. Our regression rate is closer to 3.23 mm/sec for the same  $G_{oxavg}$  value as can be observed from Figure 7. A test using a HTPB hybrid with gaseous oxygen achieved a regression rate of only 1.54 mm/s for their test case where mass flux was 130 kg/m<sup>2</sup>-s.<sup>6</sup> Regression rates of this size are typical for HTPB. Our increased regression rate can partly be attributed to our choice of oxidizer. The method of heat transfer to the fuel from the flame zone is much stronger due to our high temperatures.

Two reasons caused some difficulty in calculating the regression rates of the paraffin wax. First, after the test runs, the collection of the remaining wax was troublesome because some of the wax was still in its liquid state. Second, the softness of the fuel caused some slight deformation in the fuel after firing which can be seen in Figure 6. This also may have affected our web thickness measurements. To account for this uncertainty, a 5% margin for loss of sample mass after firing was assumed and these regression rates are included in Table 2.

Overall, the test was a success due mainly to the fact that our rate measuring technique yielded values higher than expected. This is likely due to the high temperatures of  $H_2O_2$  following the catalytic reaction which facilitates liquefying and droplet creation from the paraffin wax.

## References

<sup>1</sup> Karabeyoglu, M.A., Cantwell, B.J., and Altman, D., "Development and testing of paraffin-based hybrid rocket fuels," AIAA Paper A01-34608, Stanford, California, 2001.

<sup>2</sup> GuiPep, Arthur J. Lekstutis, Traxel Labs Inc., Revision 0.04

<sup>3</sup> Frederick, R. A., Moser, M. D., Knox, R. L., Josh J., “Ballistic Properties of Mixed Hybrid Propellants,” UAH Propulsion Research Center, University of Alabama in Huntsville, AL, July. 2004.

<sup>4</sup> Hill, Nicola. “Combustion of Glycidylazide Polymer Solid Fuel in a Hybrid Rocket Motor Using Hydrogen Peroxide,” USAFA, 2003.

<sup>5</sup> Humble, R. W., Henry, G. N., Larson, W. J., *Space Propulsion Analysis and Design*, Space Technology Series, McGraw-Hill Companies, Inc., 1995.

<sup>6</sup> Risha, G. A., Ulas, A., Boyer, E., Kumar, Surajit., Kuo, K., “Combustion of HTPB-Based Solid Fuels Containing Nano-Sized Energetic Powder in a Hybrid Rocket Motor,” Pennsylvania State University, AIAA 2001-3535.